nature communications

Article

https://doi.org/10.1038/s41467-025-61265-4

Superacid counteranion as flexible-coordinating ligand for asymmetric organo-bismuth catalysis

Received: 18 February 2025

Accepted: 13 June 2025

Published online: 02 July 2025

Check for updates

Jin Hyun Park[1,3], Seok Yeol Yoo[2,3], Myoung Hyeon Shin[1], Sungwook Jeong[2], Yoonsu Park[2] ✉ & Han Yong Bae[1] ✉

Asymmetric binary catalysis, particularly combining chiral Brønsted acids with Lewis acids, is an emerging strategy in synthetic chemistry. Although a few catalyst combinations exist for stereoselective transformations, their scope is generally limited to pre-organized, activated substrates. Here, we report binary catalysis combining an organosuperacid with bismuth, where the counteranion of chiral *N*-triflyl phosphoramide acts as a flexible-coordinating ligand. This system demonstrates exceptional reactivity and enantioselectivity in the asymmetric allylation of α-keto thioesters, forming enantio-enriched α-hydroxy thioesters with a tetra-substituted stereogenic carbon center (up to > 99% yield and 97% *ee*). The success is attributed to bismuth's flexibility during activation, enhancing also interactions with the thioester-tethered substrate. Integrated experimental, analytical, and computational studies highlight the unique assembly enabled by the chiral Brønsted acid and bismuth salt system.

Chiral α-hydroxy carbonyls hold significant importance as essential building blocks for fine chemicals and, more critically, for the synthesis of pharmaceuticals, where their stereochemical integrity is often crucial for biological activity (Fig. 1a). Therefore, developing efficient chemical processes for synthesizing such chiral structures has become crucial in asymmetric catalysis. Asymmetric binary catalysis can be a highly promising tool for achieving these challenging stereoselective reactions. Over the past decades, the combination of transition metals (e.g., Ti, Pd, Rh, Ag, Au, and Fe) or rare-earth metals (e.g., Yb) with chiral Brønsted acid organocatalysts has emerged as a useful approach, enabling highly efficient asymmetric transformations (Fig. 1b)[1–8]. A conventional approach to asymmetric Lewis acid catalysis comprehends utilizing chiral amine- or alcohol-modified Lewis basic ligands coordinated with metal centers, facilitated by structurally fixed, redox-neutral chiral complexes[9]. Contrary to this, binary strategy leverages the distinct activation modes of each component efficiently and synergistically: the metal functions as a redox[1] or Lewis acidic[10] center, while the organic acid serves as a precursor for counteranion or mono-/bidentate ligand after deprotonation. Chiral phosphoric acids[11,12] (CPAs: $pK_a = 12.7$ (in MeCN, measured)[13], when (R = Ph)) have exhibited wide applicability as organic counterparts in a plethora of catalytic reactions[14–16]. Considerable catalytic activities and selectivities have been achieved by utilizing the unique metal–CPA binary platforms based on their strong coordinating abilities, which offer benefits that a sole catalyst cannot realize[17–20]. Recent studies have expanded their usage in conjunction with main group elements (e.g., Li, Al, Ca, and Mg)[10,21–23].

Bismuth (Bi) is a post-transition metal that offers a sustainable alternative to conventional metals for various applications[24–27]. Unlike other heavy metals, bismuth is cost-effective and significantly stable in aqueous environments. Additionally, it has exceptionally low toxicity—lower than that of common table salt—making it safe for use in oral medications (e.g., bismuth subcitrate: for the treatment of *Helicobacter pylori* infections[28]). Despite these advantages, only a limited number of asymmetric bismuth-based binary catalytic approaches have been disclosed in recent years. Cheng, Li, and coworkers showed the synergistic effect of Bi(III) salt and CPAs in diverse asymmetric transformations, such as 1,2-allylation reactions, kinetic resolution, and Mukaiyama–Mannich reaction[29–35]. Although these Bi–CPA binary

[1]Department of Chemistry, Sungkyunkwan University, Suwon, Republic of Korea. [2]Department of Chemistry, Korea Advanced Institute of Science and Technology (KAIST), Daejeon, Republic of Korea. [3]These authors contributed equally: Jin Hyun Park, Seok Yeol Yoo. ✉e-mail: yoonsu.park@kaist.ac.kr; hybae@skku.edu

https://doi.org/10.1038/s41467-025-61265-4

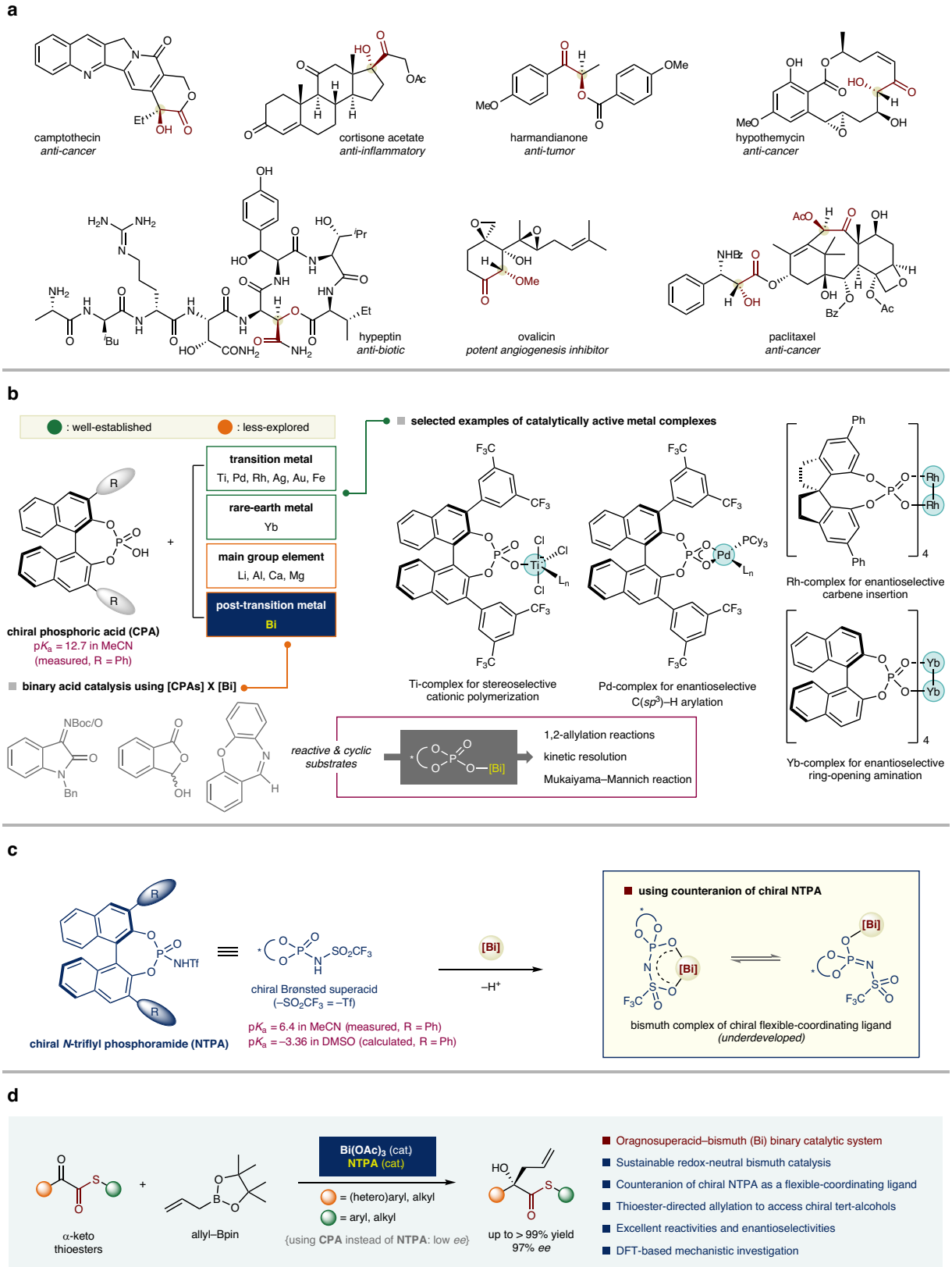

Fig. 1 | Thioester-directed asymmetric allylation via organosuperacid-bismuth binary catalysis. a Representative bioactive compounds bearing chiral α-hydroxy carbonyls with stereogenic carbon center(s). **b** Previous works: [CPAs] X [Lewis acids]. **c** Underdeveloped binary acid catalysis: [NTPA] X [Bi]. **d** This work: Thioester-directed asymmetric allylation via organic-bismuth binary acid catalysis.

Ac acetyl, Bn benzyl, Boc *tert*-butyloxycarbonyl, Bz benzoyl, Cy cyclohexyl, DFT density functional theory, DMSO dimethyl sulfoxide, *ee* enantiomeric excess, Et ethyl, ^{t}Bu isobutyl, ^{i}Pr isopropyl, L_n ligand, Me methyl, OAc acetate, Ph phenyl, Tf trifluoromethanesulfonyl (triflyl).

https://doi.org/10.1038/s41467-025-61265-4

Table 1 | Optimization of chiral acid organocatalyst

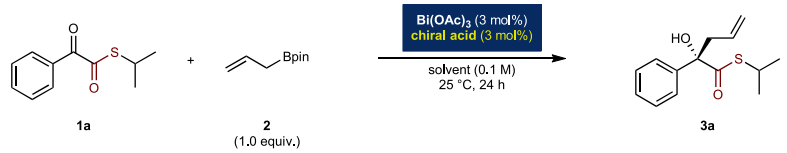

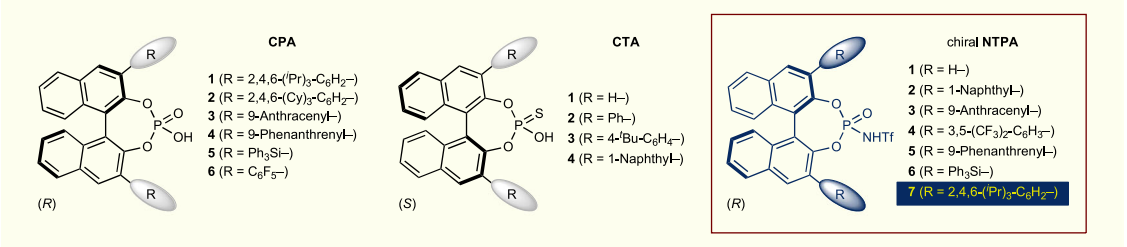

Entry[a]	Chiral acid	Solvent	Yield (%)[b]	ee (%)[c]
1	**CPA-1**	CH_2Cl_2	56	27
2	**CPA-2**	CH_2Cl_2	>99	42
3	**CPA-3**	CH_2Cl_2	>99	39 (*ent*)
4	**CPA-4**	CH_2Cl_2	82	14 (*ent*)
5	**CPA-5**	CH_2Cl_2	98	16
6	**CPA-6**	CH_2Cl_2	82	13 (*ent*)
7	**CTA-1**	CH_2Cl_2	74	6 (*ent*)
8	**CTA-2**	CH_2Cl_2	57	17
9	**CTA-3**	CH_2Cl_2	68	25
10	**CTA-4**	CH_2Cl_2	>99	61 (*ent*)
11[d]	**NTPA-1**	CH_2Cl_2	71	19 (*ent*)
12[d]	**NTPA-2**	CH_2Cl_2	>99	12
13[d]	**NTPA-3**	CH_2Cl_2	93	22 (*ent*)
14[d]	**NTPA-4**	CH_2Cl_2	>99	65
15	**NTPA-5**	CH_2Cl_2	>99	26
16	**NTPA-6**	CH_2Cl_2	60	5 (*ent*)
17[d]	**NTPA-7**	CH_2Cl_2	>99	47 (*ent*)
18	**NTPA-7**	PhCl	>99	56
19	**NTPA-7**	THF	44	35
20	**NTPA-7**	EtOAc	77	68
21	**NTPA-7**	PhMe	>99	75
22[e]	**NTPA-7**	PhMe	>99 (92)[f]	91

[a]Reaction condition: α-Keto thioester (**1a**, 0.1 mmol), allyl–Bpin (**2**, 1.0 equiv., 0.1 mmol), $Bi(OAc)_3$ (3 mol%, 0.003 mmol), chiral acid (3 mol%, 0.003 mmol), solvent (0.1 M, 1.0 mL), 25 °C, 24 h.
[b]Yield (%) was determined by ^{1}H NMR integration.
[c]Enantiomeric excess (*ee*) value was determined by chiral HPLC analysis. *ent* opposite enantiomer as major form.
[d](*S*)-Enantiomer of NTPA was used.
[e]Reaction was performed at −20 °C for 48 h.
[f]Isolated yield. Bpin boronic acid pinacol ester, ^{t}Bu *tert*-butyl, Cy cyclohexyl, ^{i}Pr isopropyl, OAc acetate, Ph phenyl, Tf trifluoromethanesulfonyl (triflyl).

systems have demonstrated remarkable success, their applications have been mainly limited to electrophiles with reactive, cyclic (rigid) imine or carbonyl backbones, such as isatin-derived *N*-protected ketimines, cyclic oxocarbenium ions, *N*-protected isatins, dibenzo[b_f][1,4]oxazepines, β,γ-unsaturated α-keto esters, and racemic 2*H*-azirines. Catalytic reactions utilizing functionalized acyclic substrates are deemed challenging, likely due to the weaker binding of substrate to the binary active site in these systems. Therefore, we hypothesized that a chiral strong Brønsted acid might be an efficient precursor for the counteranion of the elaborate system because it contains multiple transient coordinating functional atoms. This flexible coordination may promote a harmonic synergy between the complex's stability and its catalytic activity by leveraging the coordination–decoordination equilibrium[36,37]. While one part of the ligand remains firmly anchored, a weakly binding unit of the potential multidentate ligand can reversibly dissociate from the reaction center, creating an active site for substrate interaction. In this context, we envisioned that a bismuth-counteranion of chiral organosuperacid[38–40] as a ligand could pave the way for a new approach in asymmetric binary catalysis. This strategy may offer broad compatibility towards challenging substrates and achieve high levels of regio- and stereoselectivity (Fig. 1c).

Herein, we report a binary catalytic system that combines a chiral organosuperacid with a Bi(III) salt (Fig. 1d). We found that the bismuth complexes of counteranions derived from chiral *N*-triflyl phosphoramides[38,40] (NTPAs: $pK_a = 6.4$ (in MeCN, measured)[13] and $pK_a = -3.36$ (in dimethyl sulfoxide (DMSO), calculated)[41], respectively, when (R = Ph)), efficiently catalyze the enantioselective allylation reaction of α-keto thioesters. This discovery is significant because (i) the use of asymmetric binary acid catalysis employing chiral organosuperacids as flexible-coordinating ligand precursors represents an underexplored approach (with only a few chiral NTPAs documented as counteranions[42–45] or as compatible Brønsted acids[46–50] in metal

https://doi.org/10.1038/s41467-025-61265-4

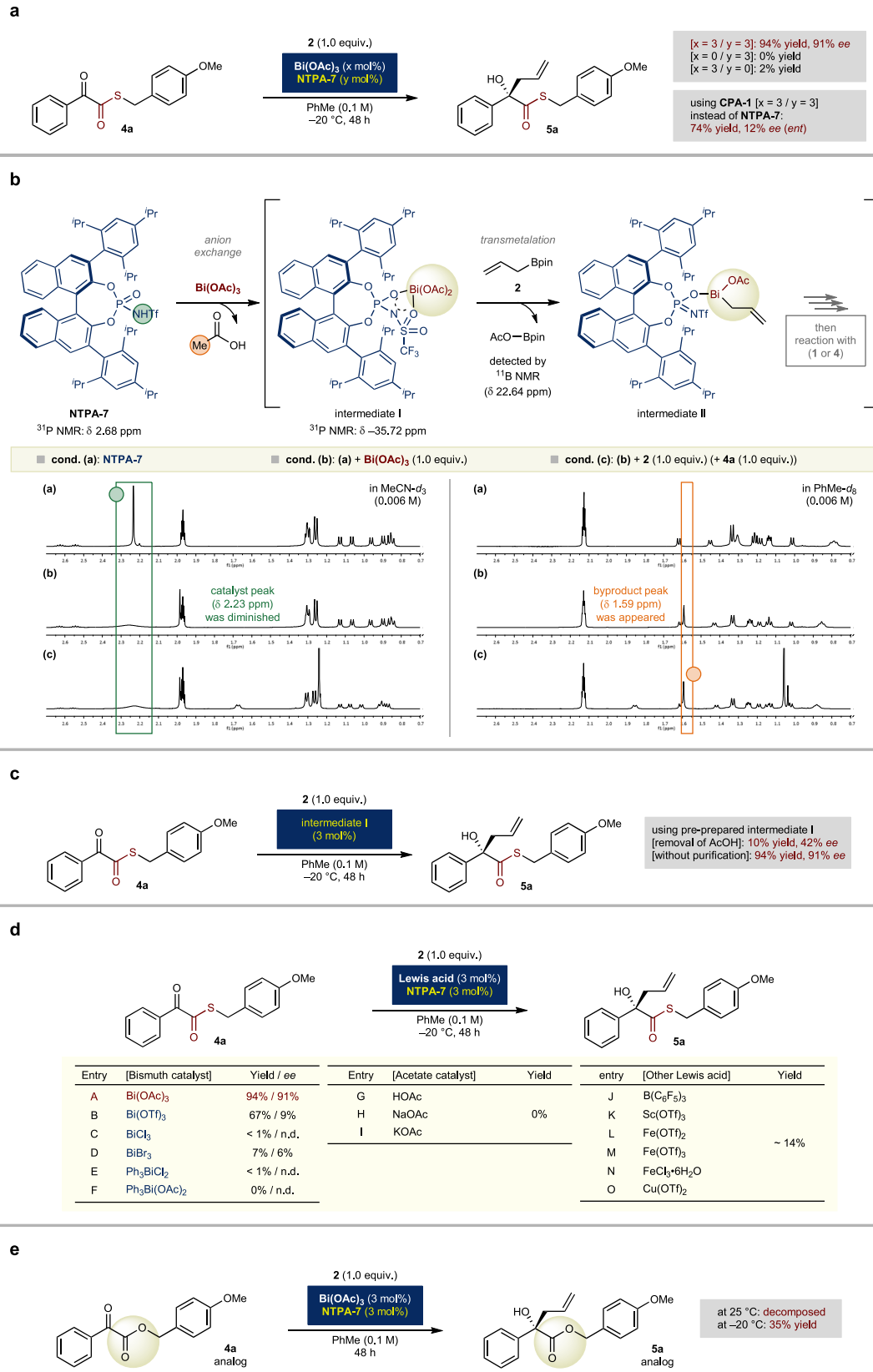

Entry	[Bismuth catalyst]	Yield / *ee*
A	$Bi(OAc)_3$	94% / 91%
B	$Bi(OTf)_3$	67% / 9%
C	$BiCl_3$	< 1% / n.d.
D	$BiBr_3$	7% / 6%
E	Ph_3BiCl_2	< 1% / n.d.
F	$Ph_3Bi(OAc)_2$	0% / n.d.

Entry	[Acetate catalyst]	Yield
G	HOAc	
H	NaOAc	0%
I	KOAc	

entry	[Other Lewis acid]	Yield
J	$B(C_6F_5)_3$	
K	$Sc(OTf)_3$	
L	$Fe(OTf)_2$	~ 14%
M	$Fe(OTf)_3$	
N	$FeCl_3{\cdot}6H_2O$	
O	$Cu(OTf)_2$	

Fig. 2 | Experimental and analytical investigations of the organosuperacid-bismuth binary catalytic system. a Control reactions for catalyst evaluation. **b** ^{1}H NMR (500 MHz) study for in situ-generated catalytic assembly. **c** Employing pre-prepared intermediate **I** as catalyst. **d** Examination of various Lewis acid catalysts and others. **e** Reaction using α-keto oxoester as starting material. [a]Yield (%) was determined by ^{1}H NMR integration. [b]Enantiomeric excess (*ee*) value was determined by chiral HPLC analysis. *ent* = opposite enantiomer as major form. Ac acetyl, Bpin boronic acid pinacol ester, ^{i}Pr isopropyl, Me methyl, OAc acetate, OMe methoxy, OTf triflate, Ph phenyl, Tf trifluoromethanesulfonyl (triflyl).

https://doi.org/10.1038/s41467-025-61265-4

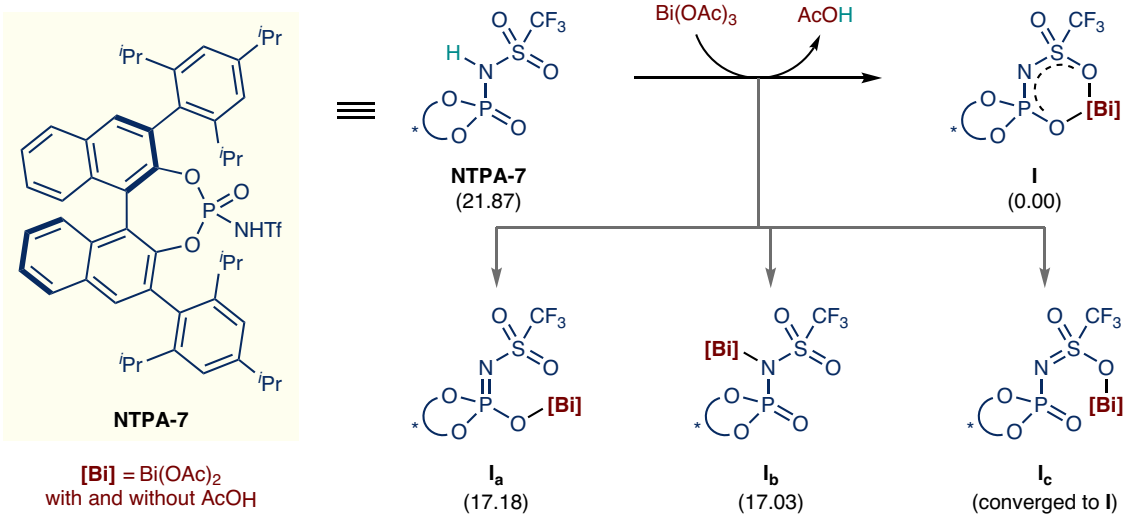

Fig. 3 | Gibbs free energies (in kcal/mol) of possible intermediates involved in the anion exchange during catalyst activation. Ac acetyl, ^{i}Pr isopropyl, OAc acetate, Tf trifluoromethanesulfonyl (triflyl).

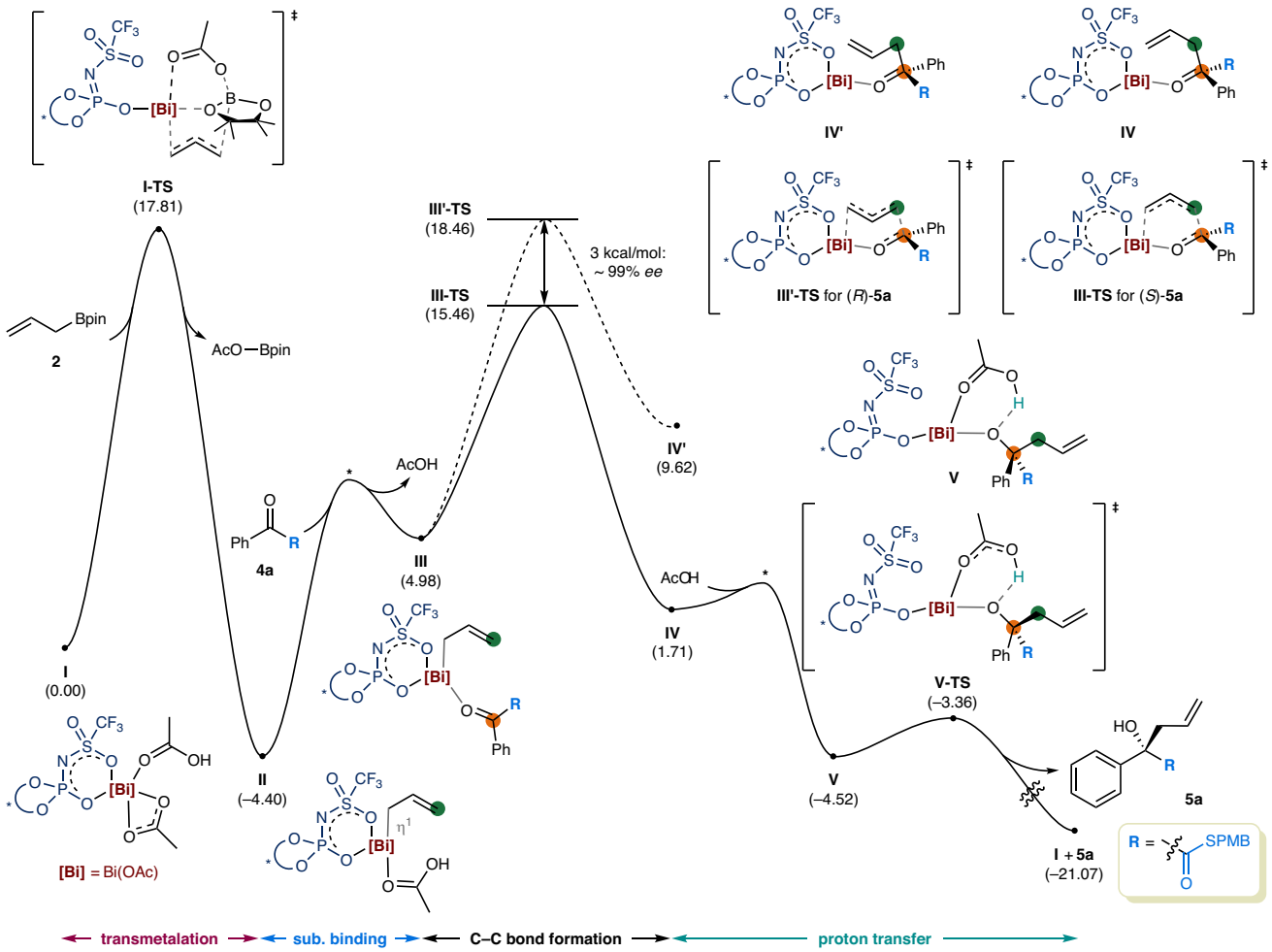

Fig. 4 | Computed energy profile of model catalytic reaction (in kcal/mol). *Transition states that were not located on their electronic energy surfaces are marked with asterisks. DFT calculations were performed at SMD(toluene) M06-2X/{6-311 + G**/def2-TZVPP for Bi}//{6-31 G**/SDD} level of theory. Ac acetyl, Bpin boronic acid pinacol ester, *ee* enantiomeric excess, OAc acetate, Ph phenyl, PMB *p*-methoxybenzyl, TS transition state.

catalysts), and (ii) the underlying mechanism of chiral induction in post-transition metals such as bismuth has been scarcely investigated owing to their complex coordination behaviors. By utilizing the distinctive binding properties of this catalytic approach, we achieved (iii) excellent enantioselectivities in challenging allylation reactions[51–55] under mild conditions, enabling the formation of thioester-tethered tetra-substituted stereogenic carbon center in a single protocol. Thioesters are highly reactive yet sufficiently stable intermediates and

https://doi.org/10.1038/s41467-025-61265-4

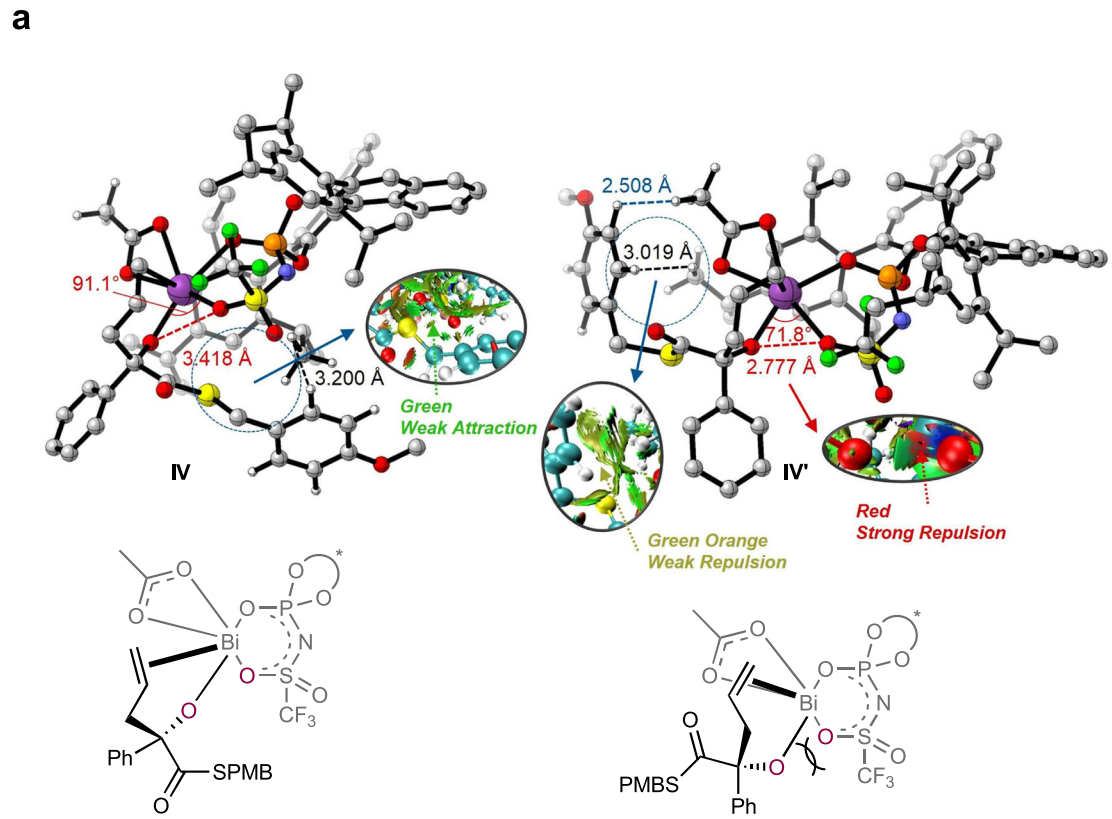

b

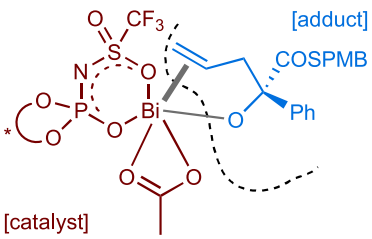

ΔE (kcal/mol)	IV	IV'	Δ(IV – IV')
Steric Interaction	–53.6	–49.4	–4.2
Orbital Interaction	–132.7	–134.5	1.8
Total Bonding Energy	–186.3	–183.9	–2.4

Fig. 5 | Structural features and energy decomposition analysis of key intermediates IV and IV′. a Structures of the enantio-determining key intermediates. **b** Energy decomposition analysis (in kcal/mol). Ph phenyl, PMB *p*-methoxybenzyl.

play a pivotal role in biology and organic synthesis, enabling key metabolic processes and further versatile chemical transformations[56]. Experimental, analytical, and computational mechanistic studies corroborated the cooperative covalent and non-covalent interactions between the Bi(III)–NTPA binary acid framework and the coordinated substrates.

Results and discussion

Catalyst evaluation

For the model reaction, we selected *S*-isopropyl α-keto thioester **1a** as the acceptor to study catalytic efficiency for acyclic substrates, underdeveloped in previous catalytic systems. Initially, we investigated the reaction between **1a** and allylboronic acid pinacol ester (allyl–Bpin, **2**), using 3 mol% of $Bi(OAc)_3$ and 1,1′-bi-2-naphthol (BINOL)-derived chiral acid organocatalyst, in CH_2Cl_2 at ambient temperature for 24 h (Table 1). By exploiting **CPA-1** (CPA featuring 3,3′-bis(2,4,6-triisopropylphenyl)-substituents), we obtained the desired chiral *S*-isopropyl α-hydroxy thioester **3a** in 56% conv., whereas with low enantioselectivity (27% *ee*, Entry 1). Other attempted CPAs did not render satisfactory results (Entries 2–6), driving us to explore alternative core structures, such as chiral thiophosphoric acids. While some promising results were obtained, the efficacy of the CTA scaffold proved to be limited (Entries 7–10).

For stronger acids like chiral NTPAs, an improvement in catalytic performance in terms of reactivity and enantioselectivity was observed (Entries 11–17). Notably, the reaction using the catalyst **NTPA-7** (chiral NTPA bearing 3,3′-bis(2,4,6-triisopropylphenyl)-substituents), brought significantly enhanced outcome compared to its CPA analog **CPA-1** (**NTPA-7**: > 99% conv. and 47% *ee* (Entry 17) *vs* **CPA-1**: 56% conv. and 27% *ee* (Entry 1)). The most dramatic enantioselectivity increment was obtained in toluene (PhMe) among the examined solvents (up to 75% *ee*, Entries 18–21). Finally, at a lowered temperature (−20 °C) for an extended reaction time (48 h), a superior result was furnished (92% yield and 91% *ee*, Entry 22). Other factors did not demonstrate a significant positive impact (see Supplementary Information for details). Although **CTA-4** and **NTPA-4** were promising candidates in the early stages, their catalytic efficacies were less consistent under various reaction conditions (see Supplementary Information for details).

https://doi.org/10.1038/s41467-025-61265-4

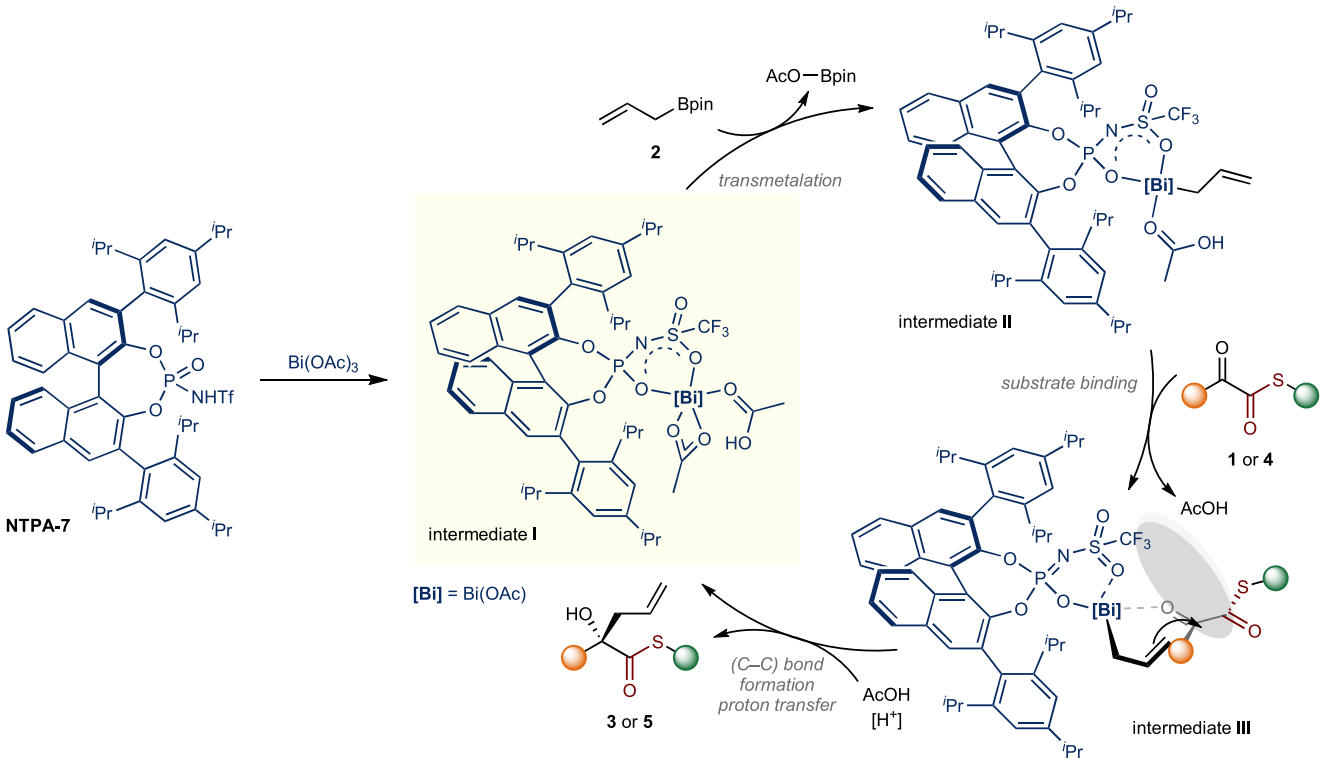

Fig. 6 | Proposed reaction mechanism for organosuperacid-bismuth binary system-catalyzed asymmetric allylation. Ac acetyl, Bpin boronic acid pinacol ester, ^{i}Pr isopropyl, OAc acetate, Tf trifluoromethanesulfonyl (triflyl).

Experimental and analytical mechanistic investigations

To gain insights into the reaction mechanism, we performed experimental and analytical studies, emphasizing the significance of the combined binary acid catalytic system. As shown in Fig. 2a, control reactions conducted with or without the catalytic components, $Bi(OAc)_3$ and **NTPA-7**, indicate that both are crucial for achieving the desired reactivity and enantioselectivity. Noticeably, the model reaction was inactive when either $Bi(OAc)_3$ or **NTPA-7** was absent (< 2 conv.). Using **CPA-1** instead of **NTPA-7** under the standard reaction condition resulted in considerably declined reactivity and enantioselectivity (74% yield and 12% *ee*). These facts indicate that the triflyl group (−Tf = $-SO_2CF_3$) at **NTPA-7** interacts with $Bi(OAc)_3$, and such synergistic action plays a critical role in efficient stereoselective catalysis.

We next carried out a series of ^{1}H NMR measurements to detect the in situ binary acid catalytic assembly (Fig. 2b). When **NTPA-7** and $Bi(OAc)_3$ were mixed, the Brønsted acid peak of **NTPA-7** immediately disappeared (δ = 2.23 ppm in MeCN-d_3) and the generation of acetic acid was simultaneously observed (δ = 1.59 ppm in PhMe-d_8), presumably through anion exchange. Furthermore, a new ^{31}P NMR signal (in PhMe-d_8) appeared at δ = −35.72 ppm (condition (b)) shifting from δ = 2.68 ppm (condition (a)), and we assigned the resulting species as a potential intermediate **I** (see Supplementary Figs. 269 and 270). When allyl–Bpin (**2**) was added to the pre-formed putative intermediate **I**, the formation of a potential intermediate **II**—through transmetalation-like step—was witnessed by the observation of a typical ^{11}B NMR signature of the concomitant byproduct, AcO–Bpin (δ = 22.64 ppm in PhMe-d_8, see Supplementary Figs. 269 and 270). These stoichiometric reactivities were consistent with computational studies (vide infra). Moreover, removing acetic acid from the reaction mixture and using the pre-prepared intermediate **I** as the catalyst substantially decreased both reactivity and enantioselectivity (Fig. 2c). This fact indicates that the generated acetic acid is essential for achieving a successful catalytic outcome.

As shown in Fig. 2d, alternative Bi(III) and Bi(V) salts, used in place of $Bi(OAc)_3$, proved ineffective under the optimized reaction condition, obtaining the product **5a** with low reactivities and poor enantioselectivities (up to <67% conv. and 9% *ee*, Entries B–F). When $Bi(OAc)_3$ was replaced by other acetates such as HOAc, NaOAc, and KOAc, no catalytic activity was observed (Entries G–I). Other main group and transition metal Lewis acids resulted in fruitless outcomes (Entries J–O). The importance of the thioester group was further evaluated by synthesizing an oxygen analog (Fig. 2e). When subjected to the standard reaction condition, α-keto oxoester, instead of **4a**, exhibited poor reactivity across a broad temperature range. This finding emphasizes the critical role of the thioester group in achieving a successful catalytic outcome (see Supplementary Fig. 268).

Mechanistic investigations by density functional theory (DFT)-based computation

To examine kinetically viable reaction mechanism, we performed computational studies based on DFT calculations as the SMD(toluene) M06-2X/{6-311 + G**/def2-TZVPP for Bi}//{6-31 G**/SDD} level of theory[57]. At the outset, we investigated the complexation between $Bi(OAc)_3$ and **NTPA-7** (Fig. 3). Our initial consideration included various possible coordination modes upon anion exchange. The results indicated that the formation of a six-membered bidentate complex **I** is highly exergonic with a driving force of 21.9 kcal/mol, and the spontaneous deprotonation that releases acetic acid as a byproduct was consistent with analytical observations by ^{1}H NMR monitoring in Fig. 2b. Other monodentate conformations ($\mathbf{I_a}$ and $\mathbf{I_b}$) were less stable than complex **I**, with energies of 17.2 and 17.0 kcal/mol, respectively. Meanwhile, intermediate $\mathbf{I_c}$, which exhibited weaker binding by the triflate portion, converged to the complex **I** during the geometry optimization process.

Having understood the stability of the six-membered-like chelated complex, we next evaluated the subsequent allylation reactivity on the substrates (Fig. 4). Initially, the pre-formed complex **I** can

https://doi.org/10.1038/s41467-025-61265-4

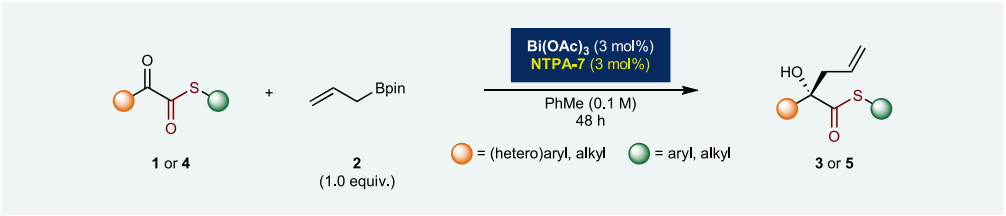

■ Various thioester substituents

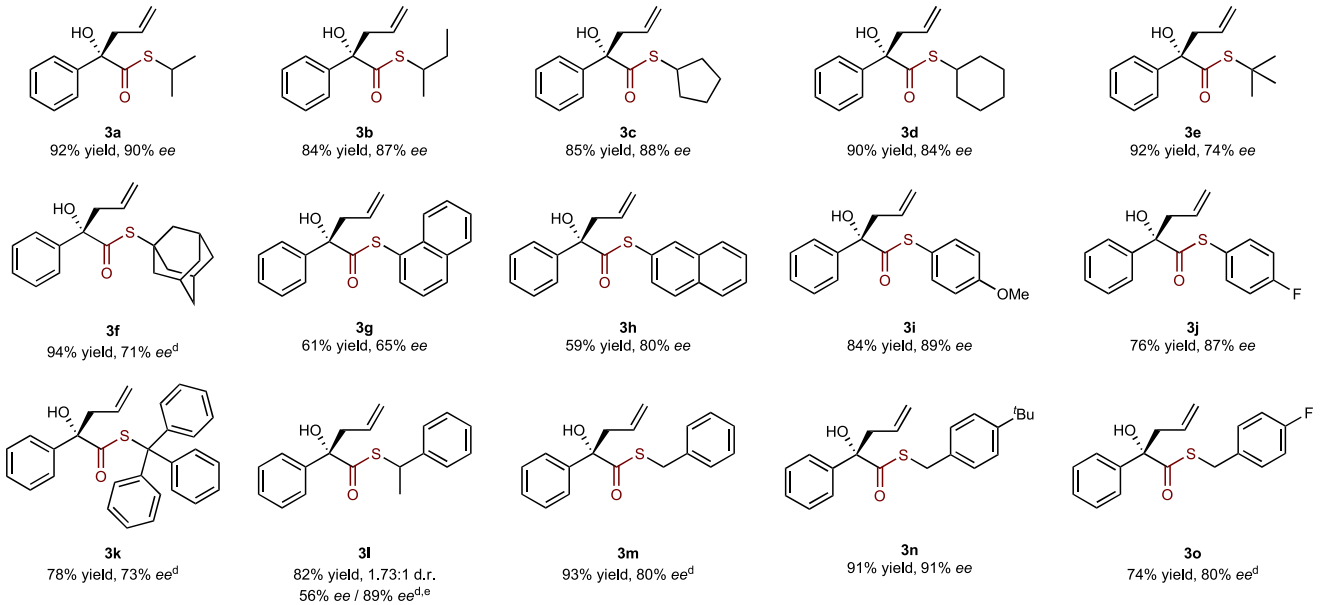

Fig. 7 | Substrate scope (continued on Fig. 8). [a]Reaction conditions: α-Keto thioesters (**1**, 0.3 mmol), allyl–Bpin (**2**, 1.0 equiv., 0.3 mmol), $Bi(OAc)_3$ (3 mol%, 0.009 mmol), **NTPA-7** (3 mol%, 0.009 mmol), PhMe (0.1 M, 3.0 mL), −20 °C, 48 h. [b]Yield (%) was determined after column chromatographic purification. [c]Enantiomeric excess (*ee*) value was determined by chiral HPLC analysis. [d]Reaction was performed at 25 °C. [e]Diastereomeric ratio (d.r.) value was determined using ^{1}H NMR analysis. Bpin boronic acid pinacol ester, Me methyl, OAc acetate, OMe methoxy, Ph phenyl.

undergo either transmetalation of allyl–Bpin (**2**) or binding of α-keto thioester **4a**. Our computational investigations on both pathways suggested that transmetalation is kinetically favored under the optimal reaction condition (see Supplementary Fig. 291). Hence, the complex **I** reacts with allyl–Bpin (**2**) through a transmetalation process, forming an allyl-bismuth complex **II** with a kinetic barrier of 17.8 kcal/mol (**I** → **I-TS**). Then, α-keto thioester **4a** binds to complex **II**, affording a catalyst–substrates complex **III**. This complex has the potential to traverse four different enantio-determining carbon–carbon (C–C) coupling transition states (see Supplementary Fig. 296), structures and energies of two representatives (**III-TS** and **III′-TS**) are displayed in Fig. 4. The transition states **III-TS** and **III′-TS** lead to the products (*S*)-**5a** and (*R*)-**5a**, respectively, where **III-TS** exhibited an activation energy that is 3.0 kcal/mol lower than that of **III′-TS**. This computational kinetic barrier for the C–C coupling aligned with our spectroscopic observation confirming the (*S*) absolute configuration. Finally, the product (*S*)-**5a** can be released through facile protonation of the resulting catalyst–adduct complex **IV** by exogenous acetic acid, facilitating the regeneration of the complex **I** to close and turn over the catalytic cycle. Attempts to explicitly locate the transition states for monotonous ligand dissociation and association were unsuccessful on electronic energy surfaces because the entropic contribution plays a critical role during these processes[58] (see Supplementary Fig. 293).

The fundamental origin of exceptional enantioselectivity was further examined by utilizing complexes **IV** and **IV′**. Electronic energy components suggested that the energy differences between **III-TS** and **III′-TS** were well-reflected in the structures of their respective resultants, **IV** and **IV′** (see Supplementary Fig. 296). As enumerated in Fig. 5a, analyzed by the non-covalent interactions (NCI) plot[59], an attractive interaction between the aryl moiety of the adduct and the ligand backbone in **IV** was revealed, showing a hydrogen–hydrogen (H–H) distance of 3.200 Å ($d_{(H-H)}$ = 3.200 Å) and an O–Bi–O angle of 91.1° ($\angle_{(O-Bi-O)}$ = 91.1°). Whereas a similar interaction was observed in **IV′**, the nature of non-covalent interaction was repulsive, due to the shorter distances between the adduct and the ligand ($d_{(H-H)}$ = 2.508 and 3.019 Å). In essence, the shorter oxygen–oxygen (O–O) distance between the adduct and the ligand in **IV′** ($d_{(O-O)}$ = 2.777 Å), along with the smaller O–Bi–O angle ($\angle_{(O-Bi-O)}$ = 71.8°), induced a strong repulsive interaction. We concluded that such interaction is substantiated in the bidentate coordination mode enabled by **NTPA-7**.

Energy decomposition analysis[60] was further conducted to quantify the unique interactions (Fig. 5b). By dividing **IV** and **IV′** into two fragments (the catalyst and the adduct, respectively), we were able to deconvolute the steric- and orbital-interaction terms using the Amsterdam Density Functional quantum chemical package[61]. The total bonding energy in **IV** is 2.4 kcal/mol lower, leading to stabilization of the complex. The steric interaction, on the other hand, contributes significantly to the energy difference of 4.2 kcal/mol, while the orbital interaction is marginal. These results underscore the influence of the bidentate ligand and non-covalent interactions, where the additional oxygen atom in **IV** plays a crucial role in differentiating the energy, and thereby affecting enantioselectivity.

Based on the mechanistic information, we propose a plausible catalytic cycle (Fig. 6). The chiral organosuperacid **NTPA-7** is readily

https://doi.org/10.1038/s41467-025-61265-4

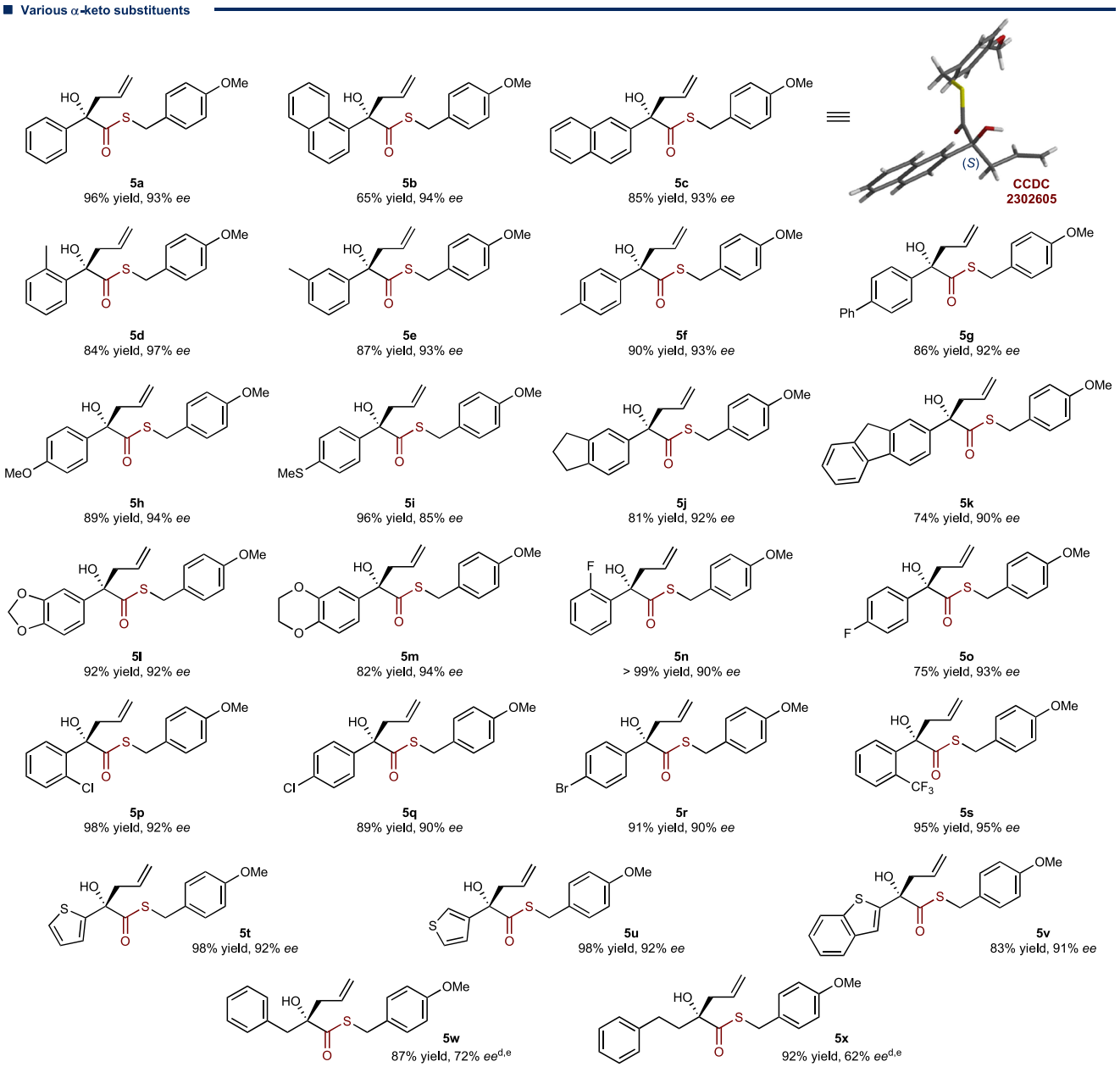

Fig. 8 | Substrate scope (continued from Fig. 7). [a]Reaction conditions: α-Keto thioesters (**4**, 0.3 mmol), allyl–Bpin (**2**, 1.0 equiv., 0.3 mmol), $Bi(OAc)_3$ (3 mol%, 0.009 mmol), **NTPA-7** (3 mol%, 0.009 mmol), PhMe (0.1 M, 3.0 mL), −20 °C, 48 h. [b]Yield (%) was determined after column chromatographic purification. [c]Enantiomeric excess (*ee*) value was determined by chiral HPLC analysis. [d]Reaction was performed at 25 °C. [e]Reaction was performed in 0.2 mmol scale. Me methyl, OMe methoxy.

activated in situ by anion exchange with $Bi(OAc)_3$, generating the active catalyst **I**. Subsequently, transmetalation of allyl–Bpin (**2**) forms the allylbismuth complex **II**, and the α-keto thioester (**1** or **4**) binds to create the adduct species **III**. After enantio-determining C–C coupling takes place to afford a tetra-substituted stereogenic carbon center, further protonation releases the chiral product (**3** or **5**) and completes the catalytic cycle.

Substrate scope

To probe the generality of the developed catalytic method, a variety of α-keto thioesters (**1** or **4**) was subjected to the optimized reaction condition (Figs. 7 and 8). Intensive modulation of thioester moiety was initially performed by varying *S*-substituents on α-keto thioesters **1** (Fig. 7). It was found that α-keto thioesters consisting of *S*-secondary alkyl substituents (**1a**–**1d**) and *S*-tertiary alkyl substituents (**1e** and **1f**) smoothly underwent the reaction, offering the corresponding chiral products (**3a**–**3f**) with high levels of reactivity (84–94% yields) and enantioselectivity (71–90% *ee*). The reaction utilizing α-keto thioesters consisting of *S*-aryl substituents with electron-donating or -withdrawing groups (**1g**–**1j**) also conducted well, attaining the corresponding chiral products (**3g**–**3j**) with moderate to good reactivities (59–84% yields) and enantioselectivities (65–89% *ee*). Encouragingly, α-keto thioesters being made up of *S*-benzyl substituents (**1k**–**1o**) were well fitted in the reaction, exhibiting the corresponding chiral products (**3k**–**3o**) with good to excellent reactivities (74–93% yields) and enantioselectivities (73–91% *ee*).

Notably, *S*-(*p*-methoxybenzyl) (*S*-PMB) α-keto thioester **4a** was identified as the optimal substrate for achieving the corresponding chiral *S*-PMB α-hydroxy thioester **5a** with notable reactivity (96% yield) and promising enantioselectivity (93% *ee*). A wide range of *S*-PMB α-keto thioesters **4** was attempted through a similar process (Fig. 8). Gratifyingly, *S*-PMB α-keto thioesters comprising of phenyl and naphthyl substituents (**4a**–**4c**), aryl substituents with electron-

https://doi.org/10.1038/s41467-025-61265-4

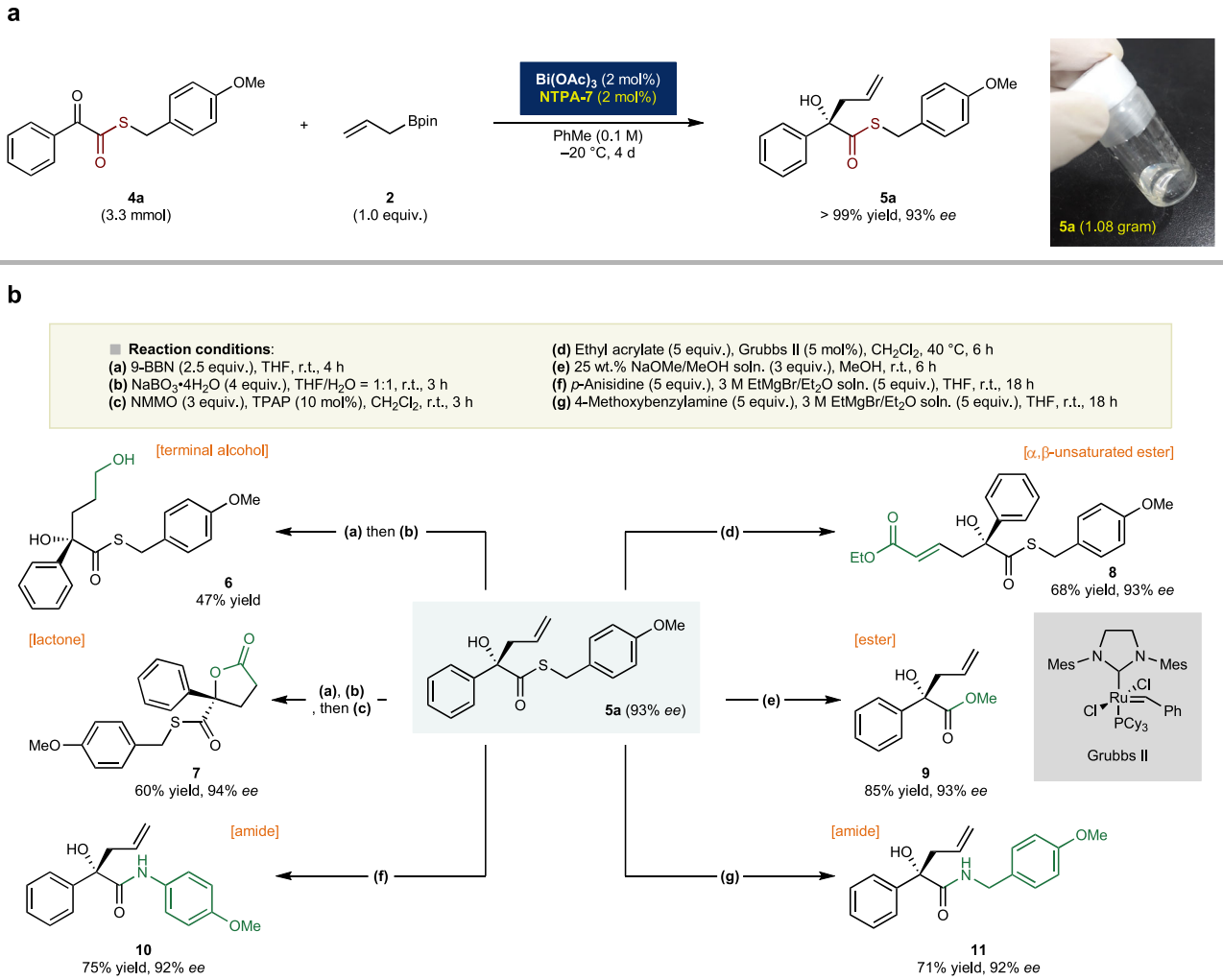

Fig. 9 | Scale-up synthesis and synthetic applications. a Scale-up synthesis. **b** Synthetic applications. 9-BBN 9-boracyclo[3.3.1]nonane, Bpin boronic acid pinacol ester, Cy cyclohexyl, *ee* enantiomeric excess, Et ethyl, Me methyl, Mes 2,4,6-trimethylphenyl (mesityl), NMMO 4-methylmorpholine *N*-oxide, OAc acetate, OMe methoxy/methoxide, Ph phenyl, THF tetrahydrofuran, TPAP tetrapropylammonium perruthenate, r.t. room temperature.

donating groups (**4d**–**4i**), and fused cyclic substituents (**4j**–**4m**) nicely underwent the reaction, furnishing the corresponding chiral products (**5a**–**5m**) with good to excellent reactivities (65–96% yields) and enantioselectivities (85–97% *ee*). Additionally, *S*-PMB α-keto thioesters comprising of aryl substituents with electron-withdrawing groups (**4n**–**4s**) and heteroaryl substituents (**4t**–**4v**) were also smoothly converted to the corresponding chiral products (**5n**–**5v**) with strikingly high levels of reactivity (75– > 99% yields) and enantioselectivity (90–95% *ee*). To our delight, it was found that the *S*-PMB α-keto thioesters comprising of alkyl substituents, such as benzyl and phenethyl groups (**4w** and **4x**, respectively), can be readily adapted to the reaction at ambient temperature, thereby creating the desired products with preeminent results ((**5w**; 87% yield and 72% *ee*) and (**5x**; 92% yield and 62% *ee*)). It should be noted that the enantioselective utilization of this type of substrate has been a challenging issue. The absolute configuration of the obtained chiral products was determined by the single crystal X-ray structure analysis. Based on the X-ray analysis of **5c**, its absolute configuration was assigned as (*S*). The absolute configuration of the other chiral products was assigned by analogy.

Synthetic applications

The feasibility of our protocol was disclosed through a gram-scale reaction of **4a**, using a reduced loading of the optimal catalytic combination (2 mol%), resulting the product **5a** without erosion of reactivity and enantioselectivity (> 99% yield and 93% *ee*, Fig. 9a). Moreover, suggested functional group derivatizations of model chiral *S*-PMB α-hydroxy thioester **5a**, while maintaining enantioselectivity, highlighted the versatility of our catalytic method (Fig. 9b). The consecutive hydroboration–oxidation of **5a** by utilizing 9-borabicyclo[3.3.1]nonane (9-BBN) was conducted to obtain the corresponding product **6** in 47% yield. The subsequent Ley–Griffith oxidation of pre-isolated **6** by utilizing 4-methylmorpholine *N*-oxide and tetrapropylammonium perruthenate gave rise to the production of a γ-lactone **7**, which constitutes a tetra-substituted stereogenic carbon center on its γ-position, in 60% yield. The olefin metathesis between **5a** and ethyl acrylate gave the corresponding product **8** in 68% yield. The transesterification of **5a** rendered the desired α-hydroxy oxoester **9** in 85% yield. In addition, the positive specific rotation of **9**, which is in accordance with (*S*) when compared with the reported values[62,63], confirmed the (*S*) absolute configuration of its precursor **5a** (see Supplementary Information for details). The coupling reagent-free direct amidation of **5a** with *p*-anisidine and 4-methoxybenzylamine gave the corresponding α-hydroxy amides **10** and **11**, respectively in 75% and 71% yield.

In summary, we developed the asymmetric organosuperacid-bismuth binary catalysis by exploiting the counteranion of chiral NTPA as a flexible-coordinating ligand. Based on the chiral redox-neutral bismuth catalytic system, we successfully achieved the

enantioselective allylation reaction of α-keto thioesters to access enantio-enriched α-hydroxy thioesters containing a tetra-substituted stereogenic carbon center with excellent reactivities and enantioselectivities (up to >99% yield and 97% *ee*). The unique features of this unexplored system, including the flexible-coordinating chiral NTPA counteranion ligand, thioester-directed catalysis, and cooperative non-covalent interactions, were highlighted through an in-depth examination of the underlying reaction mechanism. Our future works will aim to develop a broader range of bismuth-catalyzed sustainable reactions that utilize various organic acid catalysts, challenging systems accelerated by water as a reaction medium[64]. We hope this organic-bismuth binary acid system will establish a pioneering approach in the asymmetric catalysis community, unlocking new reactivity and selectivity that have not been explored earlier.

Methods

General procedure for the catalytic enantioselective allylation reaction

In a flame-dried capped test tube, equipped with a magnetic stirring bar and filled with Ar gas, $Bi(OAc)_3$ (3 mol%, 0.009 (or 0.006) mmol), **NTPA-7** (3 mol%, 0.009 (or 0.006) mmol), and PhMe (anhydrous, 0.2 M, 1.5 (or 1) mL) were added. The reaction mixture then sealed to stir to −20 °C (@ constant temperature bath) for 0.5 h. Subsequently, allyl–Bpin (**2**, 1 equiv., 0.3 (or 0.2) mmol) was added to the reaction mixture (dropwise), then sealed to stir at −20 °C for 5 min. To the crude mixture at −20 °C, *S*-PMB α-keto thioester (**1** or **4**, 0.3 (or 0.2) mmol, in PhMe (anhydrous, 0.2 M, 1.5 (or 1) mL)) was added (dropwise), then sealed to stir at −20 °C (@ constant temperature bath (or rt)) for 48 h. The resulting mixture was concentrated in vacuo, and the residue was purified by column chromatography on silica gel (EtOAc:hexanes = 1:50 to 1:3 v/v) to afford corresponding chiral *S*-PMB α-hydroxy thioester (**3** or **5**). The NMR spectra and the mass data were obtained using the Bruker Ascend™ 500 spectrometer and the Xevo G2-XS QTof mass spectrometer (combined in supercritical fluid chromatography (SFC; quadrupole TOF analyzer; Waters, Milford, MA, USA)), respectively, at the Chiral Material Core Facility Center of Sungkyunkwan University.

Data availability

All relevant data are presented in the main article and/or the Supplementary Information. CCDC 2302605 contains the supplementary crystallographic data for this paper. These data can be obtained free of charge via www.ccdc.cam.ac.uk/data_request/cif, or by emailing data_request@ccdc.cam.ac.uk, or by contacting The Cambridge Crystallographic Data Centre, 12 Union Road, Cambridge CB2 1EZ, UK; fax: +44 1223 336033. Source data are provided with the manuscript. Other data are available from corresponding author upon request. Source data are provided with this paper.

References

1. Mayer, S. & List, B. Asymmetric counteranion-directed catalysis. *Angew. Chem. Int. Ed.* **45**, 4193–4195 (2006).
2. Shao, Z. & Zhang, H. Combining transition metal catalysis and organocatalysis: a broad new concept for catalysis. *Chem. Soc. Rev.* **38**, 2745–2755 (2009).
3. Du, Z. & Shao, Z. Combining transition metal catalysis and organocatalysis – an update. *Chem. Soc. Rev.* **42**, 1337–1378 (2013).
4. Chen, D.-F., Han, Z.-Y., Zhou, X.-L. & Gong, L.-Z. Asymmetric organocatalysis combined with metal catalysis: concept, proof of concept, and beyond. *Acc. Chem. Res.* **47**, 2365–2377 (2014).
5. Yang, L., Melot, R., Neuburger, M. & Baudoin, O. Palladium(0)-catalyzed asymmetric C(sp^3)–H arylation using a chiral binol-derived phosphate and an achiral ligand. *Chem. Sci.* **8**, 1344–1349 (2017).
6. Luo, W. et al. Asymmetric ring-opening of donor–acceptor cyclopropanes with primary arylamines catalyzed by a chiral heterobimetallic catalyst. *ACS Catal.* **9**, 8285–8293 (2019).
7. Teator, A. J. & Leibfarth, F. A. Catalyst-controlled stereoselective cationic polymerization of vinyl ethers. *Science* **363**, 1439–1443 (2019).
8. Yang, L.-L. et al. Enantioselective diarylcarbene Insertion into Si–H bonds induced by electronic properties of the carbenes. *J. Am. Chem. Soc.* **142**, 12394–12399 (2020).
9. Lacour, J. & Linder, D. A counterion strategy. *Science* **317**, 462–463 (2007).
10. Hatano, M., Moriyama, K., Maki, T. & Ishihara, K. Which is the actual catalyst: chiral phosphoric acid or chiral calcium phosphate? *Angew. Chem. Int. Ed.* **49**, 3823–3826 (2010).
11. Akiyama, T., Itoh, J., Yokota, K. & Fuchibe, K. Enantioselective Mannich-type reaction catalyzed by a chiral brønsted acid. *Angew. Chem. Int. Ed.* **43**, 1566–1568 (2004).
12. Uraguchi, D. & Terada, M. Chiral brønsted acid-catalyzed direct Mannich reactions via electrophilic activation. *J. Am. Chem. Soc.* **126**, 5356–5357 (2004).
13. Kaupmees, K., Tolstoluzhsky, N., Raja, S., Rueping, M. & Leito, I. On the acidity and reactivity of highly effective chiral brønsted acid catalysts: establishment of an acidity scale. *Angew. Chem. Int. Ed.* **52**, 11569–111572 (2013).
14. Akiyama, T. Stronger brønsted acids. *Chem. Rev.* **107**, 5744–5758 (2007).
15. Parmar, D., Sugiono, E., Raja, S. & Rueping, M. Complete field guide to asymmetric BINOL-phosphate derived brønsted acid and metal catalysis: history and classification by mode of activation; brønsted acidity, hydrogen bonding, ion pairing, and metal phosphates. *Chem. Rev.* **114**, 9047–9153 (2014).
16. Akiyama, T. & Mori, K. Stronger brønsted acids: recent progress. *Chem. Rev.* **115**, 9277–9306 (2015).
17. Rueping, M., Koenigs, R. M. & Atodiresei, I. Unifying metal and brønsted acid catalysis—concepts, mechanisms, and classifications. *Chem. Eur. J.* **16**, 9350–9365 (2010).
18. Fang, G.-C., Cheng, Y.-F., Yu, Z.-L., Li, Z.-L. & Liu, X.-Y. Recent advances in first-row transition metal/chiral phosphoric acid combined catalysis. *Top. Curr. Chem.* **377**, 23 (2019).
19. Brodt, N. & Niemeyer, J. Chiral organophosphates as ligands in asymmetric metal catalysis. *Org. Chem. Front.* **10**, 3080–3109 (2023).
20. Mahlau, M. & List, B. Asymmetric counteranion-directed catalysis: concept, definition, and applications. *Angew. Chem. Int. Ed.* **52**, 518–533 (2013).
21. Hatano, M., Ikeno, T., Matsumura, T., Torii, S. & Ishihara, K. Chiral lithium salts of phosphoric acids as Lewis acid–base conjugate catalysts for the enantioselective cyanosilylation of ketones. *Adv. Synth. Catal.* **350**, 1776–1780 (2008).
22. Yue, T., Wang, M.-X., Wang, D.-X., Masso, G. & Zhu, J. Catalytic asymmetric passerini-type reaction: chiral aluminum–organo phosphate-catalyzed enantioselective α-addition of isocyanides to aldehydes. *J. Org. Chem.* **74**, 8396–8399 (2009).
23. Lv, J., Li, X., Zhong, L., Luo, S. & Cheng, J.-P. Asymmetric binary-acid catalysis with chiral phosphoric acid and MgF_2: catalytic enantioselective Friedel–Crafts reactions of β,γ-unsaturated α-ketoesters. *Org. Lett.* **12**, 1096–1099 (2010).
24. Ollevier, T. New trends in bismuth-catalyzed synthetic transformations. *Org. Biomol. Chem.* **11**, 2740–2755 (2013).
25. Moon, H. W. & Cornella, J. Bismuth redox catalysis: an emerging main-group platform for organic synthesis. *ACS Catal.* **12**, 1382–1393 (2022).
26. Mato, M. & Cornella, J. Bismuth in radical chemistry and catalysis. *Angew. Chem. Int. Ed.* **63**, e202315046 (2024).

27. Pramanik, M., Guerzoni, M. G., Richards, E. & Melen, R. L. Recent advances in asymmetric catalysis using p-block elements. *Angew. Chem. Int. Ed.* **63**, e202316461 (2024).
28. Lambert, J. R. & Midolo, P. The actions of bismuth in the treatment of Helicobacter pylori infection. *Aliment. Pharmacol. Ther.* **11**, 27–33 (1997).
29. Wang, J. et al. Bi(III)-catalyzed enantioselective allylation reactions of ketimines. *iScience* **16**, 511–523 (2019).
30. Pan, Y.-L. et al. Enantioselective allylation of oxocarbenium ions catalyzed by $Bi(OAc)_3$/chiral phosphoric acid. *ACS Catal.* **10**, 8069–8076 (2020).
31. Wang, J. et al. $Bi(OAc)_3$/chiral phosphoric acid catalyzed enantioselective allylation of isatins. *Chem. Commun.* **56**, 261–264 (2020).
32. Cai, L., Pan, Y.-L., Chen, L., Cheng, J.-P. & Li, X. $Bi(OAc)_3$/chiral phosphoric acid catalyzed enantioselective allylation of seven-membered cyclic imines, dibenzo[*b*,*f*][1,4]oxazepines. *Chem. Commun.* **56**, 12383–12386 (2020).
33. Pan, Y.-L. et al. Kinetic resolution of 2*H*-azirines by asymmetric allylation reactions. *ACS Catal.* **11**, 13752–13760 (2021).
34. Liu, X.-S., Li, Y. & Li, X. $Bi(OAc)_3$/chiral phosphoric acid-catalyzed enantioselective 1,2- and formal 1,4-allylation reaction of *β*,*γ*-unsaturated α-ketoesters. *Org. Lett.* **23**, 9128–9133 (2021).
35. Pan, Y.-L. et al. Asymmetric difluorocarbonylation reactions of non-active imines catalyzed by $Bi(OAc)_3$/chiral phosphoric acid. *Org. Chem. Front.* **9**, 3990–3997 (2022).
36. Bassetti, M. Kinetic evaluation of ligand hemilability in transition metal complexes. *Eur. J. Inorg. Chem.* **2006**, 4473–4482 (2006).
37. Elsby, M. R. & Baker, R. T. Strategies and mechanisms of metal–ligand cooperativity in first-row transition metal complex catalysts. *Chem. Soc. Rev.* **49**, 8933–8987 (2020).
38. Nakashima, D. & Yamamoto, H. Design of chiral *N*-Triflyl phosphoramide as a strong chiral brønsted acid and its application to asymmetric Diels–Alder reaction. *J. Am. Chem. Soc.* **128**, 9626–9627 (2006).
39. Cheon, C. H. & Yamamoto, H. Super brønsted acid catalysis. *Chem. Commun.* **47**, 3043–3056 (2011).
40. Caballero-García, G. & Goodman, J. M. *N*-Triflylphosphoramides: highly acidic catalysts for asymmetric transformations. *Org. Biomol. Chem.* **19**, 9565–9618 (2021).
41. Yang, C., Xue, X.-S., Li, X. & Cheng, J.-P. Computational study on the acidic constants of chiral brønsted acids in dimethyl sulfoxide. *J. Org. Chem.* **79**, 4340–4351 (2014).
42. Rueping, M. & Koenigs, R. M. Brønsted acid differentiated metal catalysis by kinetic discrimination. *Chem. Commun.* **47**, 304–306 (2011).
43. Knipe, P. C. & Smith, M. D. Enantioselective one-pot synthesis of dihydroquinolones *via* BINOL-derived Lewis acid catalysis. *Org. Biomol. Chem.* **12**, 5094–5097 (2014).
44. Bai, J.-F., Sasagawa, H., Yurino, T., Kano, T. & Maruoka, K. In situ generation of *N*-Boc-protected alkenyl imines: controlling the *E*/*Z* geometry of alkenyl moieties in the Mukaiyama–Mannich reaction. *Chem. Commun.* **53**, 8203–8206 (2017).
45. Franchino, A., Martí, À. & Echavarren, A. M. H-bonded counterion-directed enantioselective Au(I) Catalysis. *J. Am. Chem. Soc.* **144**, 3497–3509 (2022).
46. Han, Z.-Y. et al. Hybrid metal/organo relay catalysis enables enynes to be latent dienes for asymmetric Diels–Alder reaction. *J. Am. Chem. Soc.* **134**, 6532–6535 (2012).
47. Wang, P.-S. et al. Enantioselective relay catalytic cascade intramolecular hydrosiloxylation and Mukaiyama aldol reaction. *Chem. Eur. J.* **19**, 6234–6238 (2013).
48. Wu, X., Li, M.-L. & Wang, P. Hybrid gold/chiral brønsted acid relay catalysis allows an enantioselective synthesis of (−)-5-*epi*-Eupomatilone-6. *J. Org. Chem.* **79**, 419–425 (2014).
49. Li, N., Chen, D.-F., Wang, P.-S., Han, Z.-Y. & Gong, L.-Z. Relay catalytic cascade hydrosiloxylation and asymmetric hetero-Diels – Alder reaction. *Synthesis* **46**, 1355–1361 (2014).
50. Zhao, P. et al. Asymmetric intramolecular hydroalkoxylation of unactivated alkenes catalyzed by chiral *N*-triflyl phosphoramide and $TiCl_4$. *Chin. J. Chem.* **38**, 565–569 (2020).
51. Kennedy, J. W. J. & Hall, D. G. Recent advances in the activation of boron and silicon reagents for stereocontrolled allylation reactions. *Angew. Chem. Int. Ed.* **42**, 4732–4739 (2003).
52. Denmark, S. E. & Fu, J. Catalytic enantioselective addition of allylic organometallic reagents to aldehydes and ketones. *Chem. Rev.* **103**, 2763–2793 (2003).
53. Marek, I. & Sklute, G. Creation of quaternary stereocenters in carbonyl allylation reactions. *Chem. Commun*. 1683–1691 https://doi.org/10.1039/B615042J (2007).
54. Yus, M., González-Gómez, J. C. & Foubelo, F. Diastereoselective allylation of carbonyl compounds and imines: application to the synthesis of natural products. *Chem. Rev.* **111**, 5595–5698 (2013).
55. Huo, H.-X., Duvall, J. R., Huang, M.-Y. & Hong, R. Catalytic asymmetric allylation of carbonyl compounds and imines with allylic boronates. *Org. Chem. Front.* **1**, 303–320 (2014).
56. Schnepel, C. et al. Thioester-mediated biocatalytic amide bond synthesis with in situ thiol recycling. *Nat. Catal.* **6**, 89–99 (2023).
57. Zhao, Y. & Truhlar, D. G. The M06 suite of density functionals for main group thermochemistry, thermochemical kinetic, noncovalent interactions, excited states, and transition elements: two new functionals and systematic testing of four M06-class functionals and 12 other functionals. *Theor. Chem. Acc.* **120**, 215–241 (2008).
58. Ryu, H. et al. Pitfalls in computational modeling of chemical reactions and how to avoid them. *Organometallics* **37**, 3228–3239 (2018).
59. Contreras-García, J. et al. NCIPLOT: a program for plotting noncovalent interaction regions. *J. Chem. Theory Comput.* **7**, 625–632 (2011).
60. Kitaura, K. & Morokuma, K. A new energy decomposition scheme for molecular interactions within the Hartree-Fock approximation. *Int. J. Quantum Chem.* **10**, 325–340 (1976).
61. Te Velde, G. et al. Chemistry with ADF. *J. Comput. Chem.* **22**, 931–967 (2001).
62. Ooi, T., Fukumoto, K. & Maruoka, K. Construction of enantiomerically enriched tertiary α-hydroxycarboxylic acid derivatives by phase-transfer-catalyzed asymmetric alkylation of diaryloxazolidin-2,4-diones. *Angew. Chem. Int. Ed.* **45**, 3839–3842 (2006).
63. Zheng, K., Qin, B., Liu, X. & Feng, X. Highly enantioselective allylation of α-ketoesters catalyzed by N,N′-dioxide–In(III) complexes. *J. Org. Chem.* **72**, 8478–8483 (2007).
64. Kitanosono, T., Masuda, K., Xu, P. & Kobayashi, S. Catalytic organic reactions in water toward sustainable society. *Chem. Rev.* **118**, 679–746 (2018).

Acknowledgements

Dedicated to Prof. Dr. Choong Eui Song for his 70th birthday. The generous supports of the Ministry of Science, ICT and Future Planning of Korea (MSIT, RS-2023-00259659 and RS-2023-00219859), the Ministry of Education (MOE, National Research Facilities and Equipment Center: 2022R1A6C101A751 and 2022R1A6C102A913), and Korea Toray Fellowship are gratefully acknowledged for H.Y.B. (SKKU). This work was funded by the MSIT (2022R1F1A106268, RS-2023-00213491, RS-2024-00405261, and RS-2025-00642970); the Creative Research Program and the KAIST Cross-Generation Collaborative Lab Project at KAIST to Y.P. We thank the Center for Catalytic Hydrocarbon Functionalizations at the Institute for Basic Science in Korea for allowing the use of computational resources. This work was supported by the Sungkyunkwan University and the BK21 FOUR (Graduate School Innovation) funded by the MOE, and National Research Foundation of Korea.

Author contributions

Y.P. and H.Y.B. administrated the project. J.H.P. and M.H.S. conducted the conceptualization, experiments, and analytical investigations. S.Y.Y. and S.J. conducted the computational studies and data processing. All authors involved in discussions and writing–editing the manuscript.

Competing interests

The authors declare no competing interests.

Additional information

Supplementary information The online version contains supplementary material available at https://doi.org/10.1038/s41467-025-61265-4.

Correspondence and requests for materials should be addressed to Yoonsu Park or Han Yong Bae.

Peer review information *Nature Communications* thanks Lili Zhao and the other, anonymous, reviewer(s) for their contribution to the peer review of this work. A peer review file is available.